ETH
Eidgenössische Technische Hochschule Zürich
Swiss Federal Institute of Technology Zurich

Seminar for Applied Mathematics SAM

Trefftz Co-chain Calculus

D. Casati and L. Codecasa and R. Hiptmair and F. Moro

Research Report No. 2019-19
April 2019

Seminar für Angewandte Mathematik
Eidgenössische Technische Hochschule
CH-8092 Zürich
Switzerland

Funding SNF: 2000021_165674/1

Machine Copy for Proofreading, 2019

Trefftz Co-chain Calculus

Daniele Casati*, [1], Lorenzo Codecasa[2], Ralf Hiptmair[1], and Federico Moro[3]

Abstract—The framework of co-chain calculus accommodates both finite element exterior calculus and discrete exterior calculus. It relies on volume meshes and is therefore confined to bounded domains.

In this framework we propose a way to obtain systems of equations that discretize linear stationary or time-harmonic elliptic problems on unbounded domains. This is achieved by coupling any method that fits co-chain calculus with Trefftz methods, which are based on functions that solve the homogeneous equations exactly in the unbounded complement of the meshed domain, while satisfying suitable conditions at infinity.

An example of a Trefftz method is the Multiple Multipole Program (MMP), which makes use of multipoles, i.e. solutions spawned by point sources with central singularities that are placed outside the domain of approximation. In our method the degrees of freedom describing these sources can be eliminated by a Schur complement approach, therefore leading to a boundary term for co-chain calculus that takes into account the exterior problem.

We specialize this general framework for the cell method, a particular variant of co-chain calculus, and couple it with MMP to solve frequency-domain eddy current problems. A numerical example shows the effectiveness of this approach.

1. INTRODUCTION

The framework of *co-chain calculus* [1, 2] allows for a unified treatment of a wide class of finite element and finite volume schemes, building on the foundation established by other works like [3]. This framework is the generalization of both *Finite Element Exterior Calculus* (FEEC) [4] and *Discrete Exterior Calculus* (DEC) [5]. The degrees of freedom of the former are coefficients of an expansion in terms of piecewise polynomials built on a mesh: what one obtains is a function approximating the unknown in the chosen functional space, in the way of *Finite Element Methods* (FEM). Conversely, DEC returns evaluations of the unknown on entities of (primal and dual) meshes, something more akin to finite difference or finite volume methods.

The starting point of co-chain calculus is a linear stationary or time-harmonic elliptic boundary value problem, expressed in terms of differential forms and which involves *Hodge operators* (see section 2). In this model we distinguish between *equilibrium equations*, stated by means of the exterior derivative, and *constitutive equations*, based on Hodge operators. The former are preserved exactly in the discrete co-chain model, whereas the latter entail approximation.

Hodge operators can be discretized using a primary and secondary mesh on a bounded domain. Despite their names, these meshes are not necessarily related. The discrete formulation in matrix form needs to respect only a few algebraic requirements and is independent of how Hodge operators are approximated in practice: for example, no assumption on discrete function spaces is required. This is only addressed when the framework of co-chain calculus is specialized into a numerical method.

If the quantities of interest of the method are defined on either the primary or secondary mesh, we disregard the other mesh and obtain FEEC. Conversely, some quantities of interest may be represented

Received date

* Corresponding author: Daniele Casati (daniele.casati@sam.math.ethz.ch).

[1] Seminar for Applied Mathematics, ETH Zurich, Switzerland. [2] Dipartimento di Elettronica, Informazione e Bioingegneria, Politecnico di Milano, Italy. [3] Dipartimento di Ingegneria Industriale, Università degli Studi di Padova, Italy.

Abbreviations. FEEC: Finite Element Exterior Calculus. DEC: Discrete Exterior Calculus. FEM: Finite Element Method. BEM: Boundary Element Method. MMP: Multiple Multipole Program. DtN: Dirichlet-to-Neumann.

on the primary mesh and others on the secondary mesh. In this case, a bijective relationship between the two types of unknowns is needed, which can be achieved by using a secondary mesh dual to the primary mesh. This leads to numerical schemes fitting the framework of DEC, which are called *generalized finite volume methods* in [2], *generalized finite differences* in [3], and *cell method* in [6].

1.1. Cell Method

The cell method, established by [6], relies on a pair of meshes for the spatial discretization of boundary value problems: one mesh being the dual of the other. A Delaunay–Voronoi subdivision for the dual mesh is proposed in [7], whereas barycentric dual meshes are used in [8, 9, 10].

Degrees of freedom of the cell method are integrals on entities of the primal and dual meshes. In the context of electromagnetics, where the cell method has long been used, examples are fluxes of the magnetic flux density on primal faces or line integrals of the magnetic field on dual edges [7]. This allows to rewrite differential operators applied to fields in integral form as incidence matrices between integrals on entities of the meshes, by applying Stokes' theorem [11, p. 31]. In this way, equilibrium equations can be enforced exactly.

Basis functions are required to interpolate fields locally in terms of these integral degrees of freedom and then approximate the material laws (constitutive equations). With the choice of Whitney basis functions, the matrices of FEEC can be recovered [6, 7]. Piecewise constant basis functions [12] are used in [9, 10] to interpolate on generic mesh entities (any polyhedron is allowed [13]), thus leading to more applications than FEM. Moreover, [8] overcomes some limitations of the original cell method, namely how to take into account boundary conditions and energetic quantities, by means of augmented dual meshes.

Starting from [8], the cell method has been coupled with the Boundary Element Method (BEM) for magnetostatic [9] and eddy current problems [10]. Both works end up with symmetric linear systems analogous to the one explored in this work (section 3.2), which can be handled by iterative solvers. However, those systems also contain a large, dense diagonal block due to BEM, whose inverse cannot be computed explicitly [14] if one wants to reduce the size of the final coupled system by a Schur complement approach. On the other hand, when coupled with techniques based on volume meshes, *Trefftz methods* lead to small and, for some configurations, even diagonal blocks.

1.2. Trefftz Methods

Trefftz methods seek to approximate the solution of boundary value problems on (unbounded) domains by means of global basis functions that solve the homogeneous equations of the problem exactly and satisfy suitable conditions at infinity [15].

Specifically, the *Multiple Multipole Program* (MMP) employs *multipoles*, which are solutions spawned by point sources with central singularities that are placed outside the domain of approximation [16]. This is why MMP belongs to the class of methods of auxiliary sources. In a spherical coordinate system with shifted origin, a multipole can be factored into a radial part, which includes a singularity at the new origin (the center of the multipole) and the desired behavior at infinity, and a spherical part, formulated in terms of (vector) spherical harmonics [17].

The discrete equations of a Trefftz method arise from imposing boundary conditions on hypersurfaces, and the obtained linear combination of Trefftz basis functions gives an approximate solution in the whole domain where the equations hold. The discrete equations are obtained by collocation and generally yield a badly-conditioned overdetermined system [16]. However, Trefftz functions can be made orthogonal by a change of basis [18] or by choosing them orthogonal in the first place (see section 4).

Trefftz methods have already been coupled with FEM in [19, 20] for Poisson's equation and [21] for Maxwell's equations. The coupling proposed in this work between co-chain calculus and Trefftz functions can be seen as a generalization of the *Dirichlet-to-Neumann-based* (DtN-based) *coupling* presented in [19, Section 3.2].

1.3. Outline of This Work

Section 2 presents co-chain calculus for a linear stationary or time-harmonic elliptic boundary value problem, while section 2.1 illustrates its coupling with a Trefftz method. Section 2.2 replaces the equations for the exterior problem with a simpler, but equivalent expression, given some conditions on the topology of the Trefftz domain that can always be satisfied.

Correspondingly, section 3 specializes section 2 for the cell method applied to frequency-domain eddy current problems, while section 3.1 illustrates its coupling with a Trefftz method. Section 3.2 solves the exterior problem with a magnetic scalar potential, special case of the approach of section 2.2, and gives explicit formulas for the related Trefftz functions (which are multipoles).

Finally, a numerical test based on the formulation of section 3.2 is reported in section 4.

2. CO-CHAIN CALCULUS FOR ELLIPTIC BOUNDARY VALUE PROBLEMS

We write $\Lambda^l(\mathbb{R}^n)$ for the space of differential forms of order l, $0 \leq l \leq n$, on the n-dimensional Euclidean space $\mathbb{R}^n$, $n \in \mathbb{N}$ [4, p. 13, Section 2.2]. For $l \in \{1, \ldots, n\}$ and $m := n - l$, we introduce $u \in \Lambda^{l-1}(\mathbb{R}^n)$, $\boldsymbol{\sigma} \in \Lambda^l(\mathbb{R}^n)$, $\mathbf{j} \in \Lambda^m(\mathbb{R}^n)$, $\psi \in \Lambda^{m+1}(\mathbb{R}^n)$ as differential forms of different orders on $\mathbb{R}^n$. They enter the statement of the following elliptic boundary value problem composed of two sets of equations: the equilibrium equations

$$\left\{ \begin{array}{rcl} \mathrm{d}u & = & (-1)^l \boldsymbol{\sigma} \\ \mathrm{d}\mathbf{j} & = & -\psi \end{array} \right. \tag{1a}$$

and the constitutive equations

$$\left\{ \begin{array}{rcl} \mathbf{j} & = & \star_\alpha \boldsymbol{\sigma} \\ \psi & = & \star_\gamma u \end{array} \right. \tag{1b}$$

The symbols $\star_\alpha$ and $\star_\gamma$ stand for *Hodge operators*, i.e. they supply linear mappings of l-forms into m-forms [4, p. 12], while α and γ designate Riemannian metrics on $\mathbb{R}^n$ represented by Hermitian positive-definite[†] matrix fields.

The problem is completed by the condition at infinity [22, p. 259, Theorem 8.9]

$$\|u\| = \begin{cases} C \log\|\mathbf{x}\| + \mathcal{O}\left(\|\mathbf{x}\|^{-1}\right),\ C \in \mathbb{C} & \text{if } n = 2 \\ \mathcal{O}\left(\|\mathbf{x}\|^{2-n}\right) & \text{if } n \geq 3 \end{cases} \quad \text{for } \|\mathbf{x}\| \to \infty \text{ uniformly.} \tag{2}$$

For the sake of simplicity, we consider a bounded domain $\Omega_\star$ such that, in the complement $\mathbb{R}^n \setminus \Omega_\star$, we have constant $\alpha, \gamma \in \mathbb{C}$. Let us also introduce $\Omega \supset \Omega_\star$, in whose complement $\mathbb{R}^n \setminus \Omega$ there is a known nonzero excitation $(l-1)$-form w such that $u|_{\mathbb{R}^n \setminus \Omega} = v + w$, with $v, w \in \Lambda^{l-1}(\mathbb{R}^n \setminus \Omega)$. The field w will enter the right-hand side of the system.

Furthermore, we assume that $\gamma = 0$ in $\mathbb{R}^n \setminus \Omega$, which implies $\psi|_{\mathbb{R}^n \setminus \Omega} = 0$ and $\mathrm{d}\mathbf{j}|_{\mathbb{R}^n \setminus \Omega} = 0$ from (1a) and (1b).

Next, we eliminate all other variables except for u in Ω:

$$\mathrm{d}\left(\star_\alpha \mathrm{d}u\right) = (-1)^l \mathrm{d}\left(\star_\alpha \boldsymbol{\sigma}\right) = (-1)^l \mathrm{d}\mathbf{j} = -\left(-1\right)^l \psi = -\left(-1\right)^l \star_\gamma u\,, \tag{3}$$

which can be rewritten as

$$(-1)^l \mathrm{d}\left(\star_\alpha \mathrm{d}u\right) + \star_\gamma u = 0\,. \tag{4}$$

The weak formulation of (4) is

$$\int_\Omega \left[(-1)^l \mathrm{d}\left(\star_\alpha \mathrm{d}u\right) + \star_\gamma u\right] \wedge \eta = 0 \quad \forall \eta \in \Lambda^{l-1}(\Omega)\,. \tag{5}$$

Integrating by parts [2, p. 254, (6)] yields

$$\int_\Omega \left(\star_\alpha \mathrm{d}u \wedge \mathrm{d}\eta + \star_\gamma u \wedge \eta\right) + (-1)^{l-1} \int_\Gamma \mathbf{t}\left(\star_\alpha \mathrm{d}u\right) \wedge \mathbf{t}\,\eta = 0 \quad \forall \eta \in \Lambda^{l-1}(\Omega)\,, \tag{6}$$

where $\mathbf{t} : \Lambda^l(\Omega) \to \Lambda^l(\Gamma)$ is the (tangential, Dirichlet) trace of l-forms for any $l \in \{0, \ldots, n\}$ on $\Gamma := \partial\Omega$.

[†] γ can also be expressed by a Hermitian positive-definite matrix scaled by a complex scalar, which is the case of section 3.

2.1. Coupling with Trefftz Method through an $(l-1)$-Form

We discretize Hodge operators inside Ω (approximation of constitutive equations), while we use Trefftz functions in the complement $\Omega_{\mathrm{T}} := \mathbb{R}^3 \setminus \Omega$, i.e. functions that belong to the *Trefftz space*

$$\mathcal{T}(\Omega_{\mathrm{T}}) := \Big\{ v \in \Lambda^{l-1}(\Omega_{\mathrm{T}}) : \ \mathrm{d}(\star_\alpha \mathrm{d} v) = 0\,, \ \ \alpha \in \mathbb{C}, \\ v \text{ satisfies the condition at infinity (2)} \Big\}. \tag{7}$$

Interface conditions are required between Ω and Ω_{T} [23, p. 107, Lemma 5.3]:

$$\begin{cases} \mathbf{t}\left(\star_\alpha \mathrm{d} u|_{\Omega} \right) = \mathbf{t}\left(\star_\alpha \mathrm{d} u|_{\Omega_{\mathrm{T}}} \right) & \text{on } \Gamma. \quad (8a) \\ \mathbf{t}\, u|_{\Omega} = \mathbf{t}\, u|_{\Omega_{\mathrm{T}}} \quad (8b) \end{cases}$$

From now on, with a small abuse of notation, we refer to $u|_{\Omega}$ as u. We also write $u|_{\Omega_{\mathrm{T}}} := v + w$, where $v \in \mathcal{T}(\Omega_{\mathrm{T}})$ and w is the known excitation $(l-1)$-form.

We then plug (8a) into (6) and impose (8b) weakly with test functions in $\mathcal{T}(\Omega_{\mathrm{T}})$ to obtain the system for the coupling:

$$\begin{aligned} &\text{Seek } u \in \Lambda^{l-1}(\Omega)\,,\ v \in \mathcal{T}(\Omega_{\mathrm{T}}) : \\ &\begin{cases} \int\limits_{\Omega} (\star_\alpha \mathrm{d} u \wedge \mathrm{d}\eta + \star_\gamma u \wedge \eta) + (-1)^{l-1} \int\limits_{\Gamma} \mathbf{t}\,(\star_\alpha \mathrm{d} v) \wedge \mathbf{t}\,\eta = (-1)^{l} \int\limits_{\Gamma} \mathbf{t}\,(\star_\alpha \mathrm{d} w) \wedge \mathbf{t}\,\eta \\ (-1)^{l-1} \int\limits_{\Gamma} \mathbf{t}\,(\star_\alpha \mathrm{d}\zeta) \wedge \mathbf{t}\, u - (-1)^{l-1} \int\limits_{\Gamma} \mathbf{t}\,(\star_\alpha \mathrm{d}\zeta) \wedge \mathbf{t}\, v = (-1)^{l-1} \int\limits_{\Gamma} \mathbf{t}\,(\star_\alpha \mathrm{d}\zeta) \wedge \mathbf{t}\, w \end{cases} \\ &\forall \eta \in \Lambda^{l-1}(\Omega)\,,\ \forall \zeta \in \mathcal{T}(\Omega_{\mathrm{T}})\,. \end{aligned} \tag{9}$$

We choose primary and secondary discretization meshes which can be unrelated [2, p. 250, Definition 2.2]. From now on, quantities related to the secondary mesh are tagged by a tilde. Then, with the discrete counterpart of the integration by parts formula used in (6), we can rewrite (9) in abstract algebraic form

$$\begin{cases} \left[\left(\mathbf{D}^{l-1}\right)^{\mathsf{H}} \mathbf{M}_\alpha^l \mathbf{D}^{l-1} + \mathbf{M}_\gamma^{l-1} \right] \vec{\mathbf{u}} + (-1)^{l-1} \left(\mathbf{T}_\Gamma^{l-1}\right)^{\mathsf{H}} \widetilde{\mathbf{K}}_{m,\Gamma}^{l-1} \mathbf{P}_\Gamma \vec{\mathbf{v}} = (-1)^{l} \left(\mathbf{T}_\Gamma^{l-1}\right)^{\mathsf{H}} \widetilde{\mathbf{K}}_{m,\Gamma}^{l-1} \vec{\boldsymbol{\omega}} \\ (-1)^{l-1} \mathbf{P}_\Gamma^{\mathsf{H}} \left(\widetilde{\mathbf{K}}_{m,\Gamma}^{l-1}\right)^{\mathsf{H}} \mathbf{T}_\Gamma^{l-1} \vec{\mathbf{u}} - \mathbf{M}_{\mathrm{T}} \vec{\mathbf{v}} = (-1)^{l-1} \mathbf{P}_\Gamma^{\mathsf{H}} \left(\widetilde{\mathbf{K}}_{m,\Gamma}^{l-1}\right)^{\mathsf{H}} \vec{\mathbf{w}} \end{cases} \tag{10}$$

using the following matrices:

- The *exterior derivative* matrix $\mathbf{D}^{l-1} \in \{-1, 0, 1\}^{N_l, N_{l-1}}$, with N_l number of l-dimensional entities of the primary mesh, is the incidence matrix between oriented l- and $(l-1)$-dimensional entities.
- *Mass* matrices $\mathbf{M}_\alpha^l \in \mathbb{C}^{N_l, N_l}$ and $\mathbf{M}_\gamma^{l-1} \in \mathbb{C}^{N_{l-1}, N_{l-1}}$ need to be square, Hermitian, and positive-definite[‡] [2, p. 254].
- We use a vector notation for the coefficient vector $\vec{\mathbf{u}} \in \mathbb{C}^{N_{l-1}}$, whose entries are related to integrals of $u \in \Lambda^{l-1}(\Omega)$ over the $(l-1)$-dimensional entities of the primary mesh. These integrals are regarded as *degrees of freedom*.
- The *trace* matrix $\mathbf{T}_\Gamma^{l-1} \in \{0, 1\}^{N_{l-1}^{\mathrm{bnd}}, N_{l-1}}$, with N_{l-1}^{bnd} number of $(l-1)$-dimensional primary mesh entities $\subset \Gamma$, selects the degrees of freedom on Γ.
- The *pairing* matrix $\widetilde{\mathbf{K}}_{m,\Gamma}^{l-1} \in \mathbb{C}^{N_{l-1}^{\mathrm{bnd}}, \widetilde{N}_m^{\mathrm{bnd}}}$ is a discrete representative of the $\wedge$-product $\int_\Gamma f \wedge g$, $f \in \Lambda^{l-1}(\Omega)$, $g \in \Lambda^m(\Omega)$. Pairing matrices need to fulfill the algebraic relationship [2, p. 254]

$$\widetilde{\mathbf{K}}_m^l = (-1)^{lm} (\mathbf{K}_l^m)^{\mathsf{H}} \iff \mathbf{K}_l^m = (-1)^{lm} \left(\widetilde{\mathbf{K}}_m^l\right)^{\mathsf{H}} \tag{11}$$

for any $l \in \{0, \dots, n\}$, $m := n - l$.

[‡] $\mathbf{M}_\gamma^{l-1}$ can also be a square Hermitian positive-definite matrix scaled by a complex scalar, which is the case of section 3.1.

- We call $\mathbf{P}_\Gamma \in \mathbb{C}^{\widetilde{N}_m^{\mathrm{bnd}},N_\mathrm{T}}$ *projection* matrix. Its meaning is clarified below. N_T is the dimension of the discrete Trefftz space $\mathcal{T}_n(\Omega_\mathrm{T}) \in \mathcal{T}(\Omega_\mathrm{T})$.
- $\vec{\mathbf{v}} \in \mathbb{C}^{N_\mathrm{T}}$ is the vector of expansion coefficients of $v \in \mathcal{T}_n(\Omega_\mathrm{T})$ with respect to a basis of the discrete Trefftz space.
- $\vec{\mathbf{w}} \in \mathbb{C}^{N_{l-1}^{\mathrm{bnd}}}$ and $\vec{\boldsymbol{\omega}} \in \mathbb{C}^{\widetilde{N}_m^{\mathrm{bnd}}}$ are known vectors determined by integrals of the excitation $(l-1)$-form w on $(l-1)$-entities of the primary mesh and by $\star_\alpha \mathrm{d}w$ on m-entities of the secondary mesh, respectively.
- $\mathbf{M}_\mathrm{T} \in \mathbb{C}^{N_\mathrm{T},N_\mathrm{T}}$ is the *energy* matrix in Ω_T. This interpretation is clarified in the remark below.

We deduce an expression for the projection matrix based on the discrete form of (6), which is also given in [2, p. 255, *Primary elimination*, (12)]. The left-hand side of the resulting linear system is

$$\left[\left(\mathbf{D}^{l-1}\right)^{\mathsf{H}} \mathbf{M}_\alpha^l \mathbf{D}^{l-1} + \mathbf{M}_\gamma^{l-1} + \left(\mathbf{T}_\Gamma^{l-1}\right)^{\mathsf{H}} \mathbf{M}_{\beta,\Gamma}^{l-1} \mathbf{T}_\Gamma^{l-1}\right] \vec{\mathbf{u}}\,, \tag{12}$$

where $\mathbf{M}_{\beta,\Gamma}^{l-1}$ is an abstract *boundary energy* term related to the Dirichlet-to-Neumann-operator. This abstract DtN-operator is defined by [2, p. 255, (10c)]

$$\mathbf{M}_{\beta,\Gamma}^{l-1} \mathbf{T}_\Gamma^{l-1} \vec{\mathbf{u}} := (-1)^{l-1} \widetilde{\mathbf{K}}_{m,\Gamma}^{l-1} \widetilde{\mathbf{T}}_\Gamma^m \tilde{\mathbf{j}}\,, \tag{13}$$

with $\widetilde{\mathbf{T}}_\Gamma^m \in \{0,1\}^{\widetilde{N}_m^{\mathrm{bnd}},\widetilde{N}_m}$ and $\tilde{\mathbf{j}} \in \widetilde{N}_m$ coefficient vector of the interpolant of $\mathbf{j} \in \Lambda^m(\Omega)$ on the secondary mesh. The entries of the vector $\widetilde{\mathbf{T}}_\Gamma^m \tilde{\mathbf{j}}$ correspond to entities of the secondary mesh on Γ.

If we substitute (13) into (12), we obtain the hybrid formulation

$$\left[\left(\mathbf{D}^{l-1}\right)^{\mathsf{H}} \mathbf{M}_\alpha^l \mathbf{D}^{l-1} + \mathbf{M}_\gamma^{l-1}\right] \vec{\mathbf{u}} + (-1)^{l-1} \left(\mathbf{T}_\Gamma^{l-1}\right)^{\mathsf{H}} \widetilde{\mathbf{K}}_{m,\Gamma}^{l-1} \widetilde{\mathbf{T}}_\Gamma^m \tilde{\mathbf{j}}\,. \tag{14}$$

Comparing (14) with the first line of (10), we have that

$$\mathbf{P}_\Gamma \vec{\mathbf{v}} = \widetilde{\mathbf{T}}_\Gamma^m \tilde{\mathbf{j}}\,, \tag{15}$$

i.e. $\mathbf{P}_\Gamma$ maps degrees of freedom of Trefftz functions to degrees of freedom of the secondary mesh on Γ.

The total number of degrees of freedom of the Trefftz discretization, N_T, is generally low because it can be shown that, under certain conditions, Trefftz methods enjoy exponential convergence [19, 24]. Thus, $\mathbf{M}_\mathrm{T}$ can easily be inverted by Gaussian elimination, and we can write the Schur complement of (10):

$$\begin{aligned}\left[\left(\mathbf{D}^{l-1}\right)^{\mathsf{H}} \mathbf{M}_\alpha^l \mathbf{D}^{l-1} + \mathbf{M}_\gamma^{l-1} + \left(\mathbf{T}_\Gamma^{l-1}\right)^{\mathsf{H}} \widetilde{\mathbf{K}}_{m,\Gamma}^{l-1} \mathbf{P}_\Gamma \mathbf{M}_\mathrm{T}^{-1} \mathbf{P}_\Gamma^{\mathsf{H}} \left(\widetilde{\mathbf{K}}_{m,\Gamma}^{l-1}\right)^{\mathsf{H}} \mathbf{T}_\Gamma^{l-1}\right] \vec{\mathbf{u}} = \\ (-1)^l \left(\mathbf{T}_\Gamma^{l-1}\right)^{\mathsf{H}} \widetilde{\mathbf{K}}_{m,\Gamma}^{l-1} \vec{\boldsymbol{\omega}} + \left(\mathbf{T}_\Gamma^{l-1}\right)^{\mathsf{H}} \widetilde{\mathbf{K}}_{m,\Gamma}^{l-1} \mathbf{P}_\Gamma \mathbf{M}_\mathrm{T}^{-1} \mathbf{P}_\Gamma^{\mathsf{H}} \left(\widetilde{\mathbf{K}}_{m,\Gamma}^{l-1}\right)^{\mathsf{H}} \vec{\mathbf{w}}.\end{aligned} \tag{16}$$

We compare the left-hand side of (16) with the generic discrete system (12), write

$$\mathbf{M}_{\beta,\Gamma}^{l-1} \equiv \widetilde{\mathbf{K}}_{m,\Gamma}^{l-1} \mathbf{P}_\Gamma \mathbf{M}_\mathrm{T}^{-1} \mathbf{P}_\Gamma^{\mathsf{H}} \left(\widetilde{\mathbf{K}}_{m,\Gamma}^{l-1}\right)^{\mathsf{H}}, \tag{17}$$

and associate the boundary energy term of (16) with the energy in Ω_T. More details on this association are given in the next paragraph.

Remark The system (9) can also be derived by finding a stationary point of the functional

$$\begin{aligned}\mathcal{L}(u,v) := \frac{1}{2}\int_\Omega (\star_\alpha \mathrm{d}u \wedge \mathrm{d}u + \star_\gamma u \wedge u) + \frac{1}{2}\int_{\Omega_\mathrm{T}} \star_\alpha \mathrm{d}(v+w) \wedge \mathrm{d}(v+w) + \\ (-1)^{l-1} \int_\Gamma \mathbf{t}\,[\star_\alpha \mathrm{d}(v+w)] \wedge \mathbf{t}\,u\,,\end{aligned} \tag{18}$$

with $u \in \Lambda^{l-1}(\Omega)$ and $v, w \in \mathcal{T}(\Omega_{\mathrm{T}})$, where w is the known excitation $(l-1)$-form.

The first integral in (18) expresses the energy of (4) on Ω, the second the energy on Ω_{T} (given $\gamma = 0$ in Ω_{T}). From the conditions for a stationary point of $\mathcal{L}$, we obtain the coupled problem in variational form

$$\begin{aligned}
&\text{Seek } u \in \Lambda^{l-1}(\Omega)\,,\ v \in \mathcal{T}(\Omega_{\mathrm{T}})\,:\\
&\begin{cases}
\int\limits_{\Omega} (\star_\alpha \mathrm{d}u \wedge \mathrm{d}\eta + \star_\gamma u \wedge \eta) + (-1)^{l-1} \int\limits_{\Gamma} \mathbf{t}\,(\star_\alpha \mathrm{d}v) \wedge \mathbf{t}\,\eta = (-1)^{l} \int\limits_{\Gamma} \mathbf{t}\,(\star_\alpha \mathrm{d}w) \wedge \mathbf{t}\,\eta, \\
(-1)^{l-1} \int\limits_{\Gamma} \mathbf{t}\,(\star_\alpha \mathrm{d}\zeta) \wedge \mathbf{t}\,u + \int\limits_{\Omega_{\mathrm{T}}} \star_\alpha \mathrm{d}\zeta \wedge \mathrm{d}v = \int\limits_{\Omega_{\mathrm{T}}} \star_\alpha \mathrm{d}\zeta \wedge \mathrm{d}w
\end{cases}\\
&\forall \eta \in \Lambda^{l-1}(\Omega)\,,\ \forall \zeta \in \mathcal{T}(\Omega_{\mathrm{T}})\,.
\end{aligned} \tag{19}$$

The same expression as (9) is obtained by noticing that

$$\int\limits_{\Omega_{\mathrm{T}}} \star_\alpha \mathrm{d}\zeta \wedge \mathrm{d}v = -(-1)^{l-1} \int\limits_{\Gamma} \mathbf{t}\,(\star_\alpha \mathrm{d}\zeta) \wedge \mathbf{t}\,v\,, \tag{20a}$$

$$\int\limits_{\Omega_{\mathrm{T}}} \star_\alpha \mathrm{d}\zeta \wedge \mathrm{d}w = -(-1)^{l-1} \int\limits_{\Gamma} \mathbf{t}\,(\star_\alpha \mathrm{d}\zeta) \wedge \mathbf{t}\,w\,, \tag{20b}$$

which hold by integration by parts because of $v, w \in \mathcal{T}(\Omega_{\mathrm{T}})$. Note that (20a) shows that $\mathbf{M}_{\mathrm{T}}$, which is its discrete representation, is a Hermitian positive-definite matrix, and therefore invertible, which ensures that the Schur complement system (16) exists.

2.2. Coupling with Trefftz Method through an $(m-1)$-Form

Now we exploit that $\mathrm{d}\mathbf{j} = 0$ in Ω_{T}, in order to switch to a potential representation; Ω_{T} is supposed to have trivial (simply-connected) topology. From (19) we derive a hybrid system for $u \in \Lambda^{l-1}(\Omega)$ and $\mathbf{j} \in \Lambda^{m}(\Omega_{\mathrm{T}})$ (with an abuse of notation) and introduce a potential form $\pi \in \Lambda^{m-1}(\Omega_{\mathrm{T}})$. It replaces the unknown $v \in \mathcal{T}(\Omega_{\mathrm{T}})$ in the exterior problem.

Based on (1a) and (1b), we can write that $\star_\alpha \mathrm{d}v = (-1)^{l}\,\mathbf{j}$ in Ω_{T}. (19) can therefore be rewritten as

$$\begin{aligned}
&\text{Seek } u \in \Lambda^{l-1}(\Omega)\,,\ \mathbf{j} \in \Lambda^{m}(\Omega_{\mathrm{T}})\,:\\
&\begin{cases}
\int\limits_{\Omega} (\star_\alpha \mathrm{d}u \wedge \mathrm{d}\eta + \star_\gamma u \wedge \eta) - \int\limits_{\Gamma} \mathbf{t}\,\mathbf{j} \wedge \mathbf{t}\,\eta = (-1)^{l} \int\limits_{\Gamma} \mathbf{t}\,(\star_\alpha \mathrm{d}w) \wedge \mathbf{t}\,\eta \\
-\int\limits_{\Gamma} \mathbf{t}\,\boldsymbol{\iota} \wedge \mathbf{t}\,u + \int\limits_{\Omega_{\mathrm{T}}} \boldsymbol{\iota} \wedge \star_{\alpha^{-1}} \mathbf{j} = (-1)^{l} \int\limits_{\Omega_{\mathrm{T}}} \boldsymbol{\iota} \wedge \mathrm{d}w
\end{cases}\\
&\forall \eta \in \Lambda^{l-1}(\Omega)\,,\ \forall \boldsymbol{\iota} \in \Lambda^{m}(\Omega_{\mathrm{T}})\,.
\end{aligned} \tag{21}$$

Let us take $\pi, \tau \in \Lambda^{m-1}(\Omega_{\mathrm{T}})$ such that, in Ω_{T}, $\mathbf{j} = \star_\alpha \mathrm{d}\pi$ and $\boldsymbol{\iota} = \star_\alpha \mathrm{d}\tau$. This means that the new Trefftz space of functions that solve the exterior problem exactly is

$$\begin{aligned}
\mathcal{T}(\Omega_{\mathrm{T}}) := \Big\{ & v \in \Lambda^{m-1}(\Omega_{\mathrm{T}}) :\ \mathrm{d}(\star_\alpha \mathrm{d}v) = 0\,,\ \ \alpha \in \mathbb{C}, \\
& v \text{ satisfies the condition at infinity (2)} \Big\},
\end{aligned} \tag{22}$$

where $(m-1)$-forms are used instead of $(l-1)$-forms as in (7).

System (21) then becomes

$$\begin{aligned}
&\text{Seek } u \in \Lambda^{l-1}(\Omega),\ \pi \in \mathcal{T}(\Omega_{\mathrm{T}}):\\
&\begin{cases}
\int\limits_{\Omega} (\star_\alpha \mathrm{d}u \wedge \mathrm{d}\eta + \star_\gamma u \wedge \eta) - \int\limits_{\Gamma} \mathbf{t}\,(\star_\alpha \mathrm{d}\pi) \wedge \mathbf{t}\,\eta = (-1)^l \int\limits_{\Gamma} \mathbf{t}\,(\star_\alpha \mathrm{d}w) \wedge \mathbf{t}\,\eta \\
\qquad - \int\limits_{\Gamma} \mathbf{t}\,(\star_\alpha \mathrm{d}\tau) \wedge \mathbf{t}\,u + \int\limits_{\Omega_{\mathrm{T}}} \star_\alpha \mathrm{d}\tau \wedge \mathrm{d}\pi \;= (-1)^l \int\limits_{\Omega_{\mathrm{T}}} \star_\alpha \mathrm{d}\tau \wedge \mathrm{d}w
\end{cases}\\
&\forall \eta \in \Lambda^{l-1}(\Omega),\ \forall \tau \in \mathcal{T}(\Omega_{\mathrm{T}}),
\end{aligned} \tag{23}$$

where we can replace the integrals on Ω_{T} with integrals on Γ similarly to (20).

3. TREFFTZ-COUPLED CELL METHOD FOR EDDY CURRENT PROBLEMS

We specialize the problem of section 2 for a frequency-domain eddy current problem in $\mathbb{R}^3$, which amounts to the case $l = 2$ and $m = 1$. The electromagnetic fields involved – expressed with the customary notations – are the magnetic vector potential $\mathbf{A} : \mathbb{R}^3 \to \mathbb{C}^3$, the magnetic flux density $\mathbf{B} : \mathbb{R}^3 \to \mathbb{C}^3$, the magnetic field $\mathbf{H} : \mathbb{R}^3 \to \mathbb{C}^3$, and the current density $\mathbf{j} : \mathbb{R}^3 \to \mathbb{C}^3$. They correspond to the differential forms $u \in \Lambda^1(\mathbb{R}^3)$, $\boldsymbol{\sigma} \in \Lambda^2(\mathbb{R}^3)$, $\mathbf{j} \in \Lambda^1(\mathbb{R}^3)$, $\psi \in \Lambda^2(\mathbb{R}^3)$ of section 2.

We also make use of material parameters $\nu, \sigma : \mathbb{R}^3 \to \mathbb{R}$ (reluctivity and conductivity) and $\omega \in \mathbb{R}$ (angular frequency). Written in Euclidean vector proxies for the forms [25, Section 2.2], the equilibrium equations become

$$\begin{cases} \nabla \times \mathbf{A} &= \mathbf{B} \\ \nabla \times \mathbf{H} &= \mathbf{j} \end{cases} \tag{24a}$$

and the constitutive equations

$$\begin{cases} \mathbf{H} &= \nu \mathbf{B} \\ \mathbf{j} &= -\imath\omega\sigma \mathbf{A} \end{cases} \tag{24b}$$

where $\imath$ is the imaginary unit. While $\omega \in \mathbb{R}$ is constant, the material parameters $\nu, \sigma : \mathbb{R}^3 \to \mathbb{R}$ generally vary in space. Note that ν and $-\imath\omega\sigma$ correspond to the Hodge operators $\star_\alpha$ and $\star_\gamma$ of section 2.

The problem is completed by the radiation condition [22, p. 259, Theorem 8.9]

$$\|\mathbf{A}\| = \mathcal{O}\left(\|\mathbf{x}\|^{-1}\right) \quad \text{for } \|\mathbf{x}\| \to \infty \text{ uniformly} \tag{25}$$

and the Coulomb gauge [11, p. 241, (6.21)]

$$\nabla \cdot \mathbf{A} = 0 \quad \text{in } \mathbb{R}^3. \tag{26}$$

We consider a domain $\Omega_\star$ such that, in the complement $\mathbb{R}^3 \setminus \Omega_\star$, we also have constant $\nu, \sigma \in \mathbb{R}$ ($\nu = \nu_{\mathrm{T}}$ and $\sigma = \sigma_{\mathrm{T}}$). Let us also introduce $\Omega \supset \Omega_\star$, $\Gamma := \partial\Omega$, in whose complement $\mathbb{R}^3 \setminus \Omega$ there is a known nonzero source $\mathbf{A}_0$, corresponding to the excitation $(l-1)$-form w of section 2, which is given by the *Biot–Savart law* [11, p. 180, (5.28)]:

$$\mathbf{A}_0(\mathbf{x}) := \frac{\mu_0}{4\pi} \int\limits_{\Omega_0} \frac{\mathbf{j}_0(\mathbf{x}')}{\|\mathbf{x} - \mathbf{x}'\|}\, \mathrm{d}\mathbf{x}', \tag{27}$$

where $\mu_0 = 4\pi \cdot 10^{-7}\,\mathrm{H\,m^{-1}}$ and $\mathbf{j}_0 : \mathbb{R}^3 \to \mathbb{R}^3$ is the source current with support on some bounded Ω_0 and $\nabla \cdot \mathbf{j}_0 = 0$.

Furthermore, we assume that $\sigma = 0$ in $\mathbb{R}^3 \setminus \Omega$, which implies $\mathbf{j}|_{\mathbb{R}^3 \setminus \Omega} = 0$ and $\nabla \times \mathbf{H}|_{\mathbb{R}^3 \setminus \Omega} = \mathbf{0}$ from (24a) and (24b).

Next, we eliminate all other variables except for $\mathbf{A}$ in Ω:

$$\nabla \times (\nu \nabla \times \mathbf{A}) + \imath\omega\sigma \mathbf{A} = \mathbf{0} \tag{28}$$

and leave (28) ungauged. Note that if $\omega \neq 0$ and σ is (piecewise) constant, (26) is implicit in (28).

Taking the weak form of (28), we end up with a special case of (6), which we discretize following the cell method by choosing a primal mesh $\mathcal{M}$ (and corresponding barycentric dual mesh $\widetilde{\mathcal{M}}$) in Ω.

Borrowing the notation from [8, 9, 10], we write (6) in discrete form:

$$\left(\mathbf{C}^{\mathsf{T}}\mathbf{M}_{\nu}\mathbf{C}+\imath\omega\mathbf{M}_{\sigma}\right)\vec{\mathbf{a}}+\widetilde{\mathbf{C}}_{\Gamma}\widetilde{\mathbf{h}}_{\Gamma}=0 \quad \text{in } \Omega\,, \tag{29}$$

which is a special case of the hybrid formulation (14):

- $\mathbf{C}\in\{-1,0,1\}^{N_{\text{faces}},N_{\text{edges}}}$ is the incidence matrix from edges to faces of the primal mesh $\mathcal{M}$ on Ω (*discrete curl*). It corresponds to the exterior derivative matrix $\mathbf{D}^{l-1}$ in (10).
- $\mathbf{M}_{\nu}\in\mathbb{R}^{N_{\text{faces}},N_{\text{faces}}}$ and $\mathbf{M}_{\sigma}\in\mathbb{R}^{N_{\text{edges}},N_{\text{edges}}}$ have entries $(\mathbf{M}_{\nu})_{i,j}=\int_{\Omega}\nu\left(\mathbf{x}\right)\,\mathbf{b}_i^{\text{f}}\cdot\mathbf{b}_j^{\text{f}}\,\mathrm{d}\mathbf{x}$ and $(\mathbf{M}_{\sigma})_{i,j}=\int_{\Omega}\sigma\left(\mathbf{x}\right)\,\mathbf{b}_i^{\text{e}}\cdot\mathbf{b}_j^{\text{e}}\,\mathrm{d}\mathbf{x}$, with $\mathbf{b}^{\text{f}},\mathbf{b}^{\text{e}}\in\mathbf{L}^2\left(\Omega\right)$ piecewise constant basis functions [12] that are linked to the faces and edges of $\mathcal{M}$, respectively. $\mathbf{M}_{\nu}$ and $\mathbf{M}_{\sigma}$ correspond to the mass matrices $\mathbf{M}_{\alpha}^{l}$ and $\mathbf{M}_{\gamma}^{l-1}$.
- $\vec{\mathbf{a}}\in\mathbb{C}^{N_{\text{edges}}}$ is the vector of line integrals of $\mathbf{A}$ on the edges of $\mathcal{M}$. It corresponds to vector $\vec{\mathbf{u}}$.
- $\widetilde{\mathbf{C}}_{\Gamma}\in\{-1,0,1\}^{\widetilde{N}_{\text{faces}},\widetilde{N}_{\text{edges}}^{\text{bnd}}}$ is the incidence matrix from boundary edges to faces of $\widetilde{\mathcal{M}}$ (faces of $\widetilde{\mathcal{M}}$ are related to edges of $\mathcal{M}$ because of duality). It corresponds to the matrix product $(-1)^{l-1}\left(\mathbf{T}_{\Gamma}^{l-1}\right)^{\mathsf{T}}\widetilde{\mathbf{K}}_{m,\Gamma}^{l-1}$.
- $\widetilde{\mathbf{h}}_{\Gamma}\in\mathbb{C}^{\widetilde{N}_{\text{edges}}^{\text{bnd}}}$ is the vector of line integrals of $\mathbf{H}$ on the boundary edges of $\widetilde{\mathcal{M}}$. It is a coupling term with the Trefftz domain.

3.1. Coupling with Trefftz Method through Magnetic Vector Potential

In the complement $\Omega_{\text{T}}:=\mathbb{R}^3\setminus\Omega$ we use Trefftz functions in

$$\begin{aligned}\boldsymbol{\mathcal{T}}\left(\Omega_{\text{T}}\right):=\Big\{&\mathbf{v}\in\mathbf{H}_{\text{loc}}\left(\mathbf{curl},\Omega_{\text{T}}\right):\ \nabla\times\left(\nabla\times\mathbf{v}\right)=\mathbf{0}\,,\\&\mathbf{v}\text{ satisfies the radiation condition (25)}\Big\},\end{aligned} \tag{30}$$

where $\mathbf{H}_{\text{loc}}\left(\mathbf{curl},\Omega_{\text{T}}\right):=\{\mathbf{v}\in\mathbf{H}\left(\mathbf{curl},\Omega_{\text{T}}\right):\ f\mathbf{v}\in\mathbf{H}\left(\mathbf{curl},\Omega_{\text{T}}\right)\ \ \forall f\in C_{\text{c}}^{\infty}\left(\Omega_{\text{T}}\right)\}$.

Interface conditions become

$$\begin{cases}\mathbf{n}\times\left(\nu\,\nabla\times\,\mathbf{A}|_{\Omega}\right)=\mathbf{n}\times\left(\nu_{\text{T}}\,\nabla\times\,\mathbf{A}|_{\Omega_{\text{T}}}\right) & \text{on }\Gamma,\quad (31a)\\ \mathbf{n}\times\mathbf{A}|_{\Omega}=\mathbf{n}\times\mathbf{A}|_{\Omega_{\text{T}}} & (31b)\end{cases}$$

where $\mathbf{n}$ is the normal vector on Γ pointing from Ω_{T} to Ω.

$\mathbf{A}|_{\Omega}$ is discretized by the cell method and $\mathbf{A}|_{\Omega_{\text{T}}}=\mathbf{A}_{\text{T}}+\mathbf{A}_0$, where $\mathbf{A}_{\text{T}}\in\boldsymbol{\mathcal{T}}\left(\Omega_{\text{T}}\right)$ and $\mathbf{A}_0$ is the known source (27).

We define a projection matrix $\mathbf{P}_{\Gamma}\in\mathbb{C}^{\widetilde{N}_{\text{edges}}^{\text{bnd}},N_{\text{T}}}$ such that $\mathbf{P}_{\Gamma}\vec{\mathbf{v}}=\widetilde{\mathbf{h}}_{\Gamma}$ (see (15)), with $\vec{\mathbf{v}}\in\mathbb{C}^{N_{\text{T}}}$ vector of coefficients of Trefftz functions in the discrete space $\boldsymbol{\mathcal{T}}_n\left(\Omega_{\text{T}}\right)\in\boldsymbol{\mathcal{T}}\left(\Omega_{\text{T}}\right)$ of dimension N_{T}, as follows:

$$\left(\mathbf{P}_{\Gamma}\right)_{i,j}:=\nu_{\text{T}}\int_{\ell_i}\boldsymbol{\tau}\cdot\left(\nabla\times\mathbf{v}_j\right)\,\mathrm{d}\vec{\boldsymbol{s}}, \tag{32}$$

where ℓ_i, $i=1,\ldots,\widetilde{N}_{\text{edges}}^{\text{bnd}}$, is an edge of $\widetilde{\mathcal{M}}$ on Γ, $\boldsymbol{\tau}$ its tangential vector, and $\mathbf{v}_j$, $j=1,\ldots,N_{\text{T}}$, the Trefftz basis functions in $\boldsymbol{\mathcal{T}}_n\left(\Omega_{\text{T}}\right)$.

We then plug (31a) into (29) by means of (32), impose (31b) weakly by multiplying it with $\mathbf{P}_{\Gamma}^{\mathsf{T}}\widetilde{\mathbf{C}}_{\Gamma}^{\mathsf{T}}$, and obtain the final discrete system

$$\begin{cases}\left(\mathbf{C}^{\mathsf{T}}\mathbf{M}_{\nu}\mathbf{C}+\imath\omega\mathbf{M}_{\sigma}\right)\vec{\mathbf{a}} &+& \widetilde{\mathbf{C}}_{\Gamma}\mathbf{P}_{\Gamma}\vec{\mathbf{v}} &=& \widetilde{\mathbf{C}}_{\Gamma}\widetilde{\mathbf{h}}_{0,\Gamma}\\ \mathbf{P}_{\Gamma}^{\mathsf{T}}\widetilde{\mathbf{C}}_{\Gamma}^{\mathsf{T}}\vec{\mathbf{a}} &-& \mathbf{M}_{\text{T}}\vec{\mathbf{v}} &=& \mathbf{P}_{\Gamma}^{\mathsf{T}}\vec{\mathbf{b}}_{0,\Gamma}\end{cases} \tag{33}$$

which is a special case of (10). $\widetilde{\mathbf{h}}_{0,\Gamma} \in \mathbb{R}^{\widetilde{N}^{\text{bnd}}_{\text{edges}}}$ and $\vec{\mathbf{b}}_{0,\Gamma} \in \mathbb{R}^{N^{\text{bnd}}_{\text{faces}}}$ are, respectively, the vector of line integrals of $\mathbf{H}_0 := \nu_{\text{T}} \nabla \times \mathbf{A}_0$ on boundary edges of $\widetilde{\mathcal{M}}$ and the vector of fluxes of $\mathbf{B}_0 := \nabla \times \mathbf{A}_0$ on boundary faces of $\mathcal{M}$.

Thanks to the integral expression for the general case (8), $\mathbf{M}_{\text{T}}$ has entries

$$(\mathbf{M}_{\text{T}})_{i,j} := \nu_{\text{T}} \int_{\Gamma} [\mathbf{n} \times (\nabla \times \mathbf{v}_i)] \cdot \mathbf{v}_j \, \mathrm{d}S = -\nu_{\text{T}} \int_{\Omega_{\text{T}}} (\nabla \times \mathbf{v}_i) \cdot (\nabla \times \mathbf{v}_j) \, \mathrm{d}\mathbf{x} \,, \tag{34}$$

where the second equality holds because of the definition of $\boldsymbol{\mathcal{T}}(\Omega_{\text{T}})$ (30). Finally, the Schur complement of (33) is

$$\left(\mathbf{C}^{\mathsf{T}} \mathbf{M}_{\nu} \mathbf{C} + \imath\omega \mathbf{M}_{\sigma} + \widetilde{\mathbf{C}}_{\Gamma} \mathbf{P}_{\Gamma} \mathbf{M}_{\text{T}}^{-1} \mathbf{P}_{\Gamma}^{\mathsf{T}} \widetilde{\mathbf{C}}_{\Gamma}^{\mathsf{T}}\right) \vec{\mathbf{a}} = \widetilde{\mathbf{C}}_{\Gamma} \widetilde{\mathbf{h}}_{0,\Gamma} + \widetilde{\mathbf{C}}_{\Gamma} \mathbf{P}_{\Gamma} \mathbf{M}_{\text{T}}^{-1} \vec{\mathbf{b}}_{0,\Gamma} \,. \tag{35}$$

3.2. Coupling with Trefftz Method through Magnetic Scalar Potential

We can simplify the matrices in (35) by making Ω_{T} simply connected, which is always allowed because Γ is set by the user. Hence, as a special case of section 2.2, we introduce a magnetic scalar potential ϕ in Ω_{T}, which corresponds to $\pi \in \Lambda^0(\Omega_{\text{T}})$ of section 2.2. The constitutive equations for the exterior problem become

$$\begin{cases} \mathbf{H} = \nu_{\text{T}} \nabla \phi & \text{in } \Omega_{\text{T}}, \quad (36a) \\ \nabla^2 \phi = 0 & \quad (36b) \end{cases}$$

with the radiation condition

$$\phi = \mathcal{O}\left(\|\mathbf{x}\|^{-1}\right) \quad \text{for } \|\mathbf{x}\| \to \infty \text{ uniformly.} \tag{37}$$

Interface conditions are

$$\begin{cases} \mathbf{n} \times \left(\nu \nabla \times \mathbf{A}|_{\Omega}\right) = \mathbf{n} \times \left(\nu_{\text{T}} \nabla \phi|_{\Omega_{\text{T}}}\right) & (38a) \\ \mathbf{n} \cdot \left(\nabla \times \mathbf{A}|_{\Omega}\right) = \mathbf{n} \cdot \left(\nabla \phi|_{\Omega_{\text{T}}}\right) & (38b) \end{cases} \quad \text{on } \Gamma.$$

As before, there is a known source ϕ_0 in Ω_{T} such that $\phi|_{\Omega_{\text{T}}} = \phi_{\text{T}} + \phi_0$, $\phi_{\text{T}} \in \mathcal{T}(\Omega_{\text{T}})$. The Trefftz space is

$$\begin{aligned} \mathcal{T}(\Omega_{\text{T}}) := \Big\{ & v \in H^1_{\text{loc}}(\Omega_{\text{T}}) : \ \nabla^2 v = 0 \,, \\ & v \text{ satisfies the radiation condition (37)} \Big\}. \end{aligned} \tag{39}$$

In particular we choose the Trefftz basis functions

$$v_{\mathsf{lm}}(r_{xc}, \theta_{xc}, \varphi_{xc}) = r_{xc}^{-\mathsf{l}-1} Y_{\mathsf{lm}}(\theta_{xc}, \varphi_{xc}) \,, \quad \mathsf{l} = 0, \ldots, \infty, \quad \mathsf{m} = -\mathsf{l}, \ldots, \mathsf{l}, \tag{40}$$

which fulfill the definition of multipoles given in section 1.2. Here, $(r_{xc}, \theta_{xc}, \varphi_{xc})$ are spherical coordinates ($r \in [0, \infty)$, $\theta \in [0, 2\pi)$, $\varphi \in [0, \pi]$) of the vector $\mathbf{x}_c := \mathbf{x} - \mathbf{c}$, with $\mathbf{c}$ center of the multipole. $Y_{\mathsf{lm}}(\theta, \varphi)$ are spherical harmonics [11, p. 107, Section 3.5].

Thanks to (38a), we can rewrite the projection matrix (32) as

$$\mathbf{P}_{\Gamma} := \widetilde{\mathbf{G}}_{\Gamma} \mathbf{R}_{\Gamma} \,, \quad (\mathbf{R}_{\Gamma})_{i,j} := \nu_{\text{T}} \, v_j(\widetilde{\mathbf{x}}_i) \,. \tag{41}$$

$\widetilde{\mathbf{G}}_{\Gamma} \in \{-1, 0, 1\}^{N^{\text{bnd}}_{\text{edges}}, N^{\text{bnd}}_{\text{nodes}}}$ is the incidence matrix from nodes to edges of $\widetilde{\mathcal{M}}$ on Γ. v_j, $j = 1, \ldots, N_{\text{T}}$, are the chosen multipoles (40), while $\widetilde{\mathbf{x}}_i$, $i = 1, \ldots, \widetilde{N}^{\text{bnd}}_{\text{nodes}}$, are the nodes of $\widetilde{\mathcal{M}}$ on Γ (which correspond to the centroids of the faces of $\mathcal{M}$ on Γ).

We can also rewrite the energy matrix $\mathbf{M}_{\text{T}}$ in (33) as

$$(\mathbf{M}_{\text{T}})_{i,j} := -\nu_{\text{T}} \int_{\Gamma} (\mathbf{n} \cdot \nabla v_i) \, v_j \, \mathrm{d}S = -\nu_{\text{T}} \int_{\Omega_{\text{T}}} \nabla v_i \cdot \nabla v_j \, \mathrm{d}\mathbf{x} \,. \tag{42}$$

4. NUMERICAL RESULTS

We provide a numerical example for the eddy current equations (24) with the radiation condition (25) and $\omega = 0$ in $\mathbb{R}^3$ (*magnetostatics*). This problem is solved for the magnetic vector potential $\mathbf{A}$ in Ω using the cell method and the magnetic scalar potential ϕ in Ω_{T} using multipoles (40). The source is given by (27), where $\mathbf{j}_0$ is tangential to a circular loop in Ω_{T} (which is Ω_0 in (27)), with $\|\mathbf{j}_0\| = 1000\,\mathrm{A}$.

We take the same axisymmetric domain of [10, Section V.A]: Ω is composed of

(i) $\Omega_\star$, which is a cylinder with a cylindrical hole and $\nu = 1/(2\mu_0)$, with $\mu_0 = 4\pi \cdot 10^{-7}\,\mathrm{H\,m^{-1}}$, surrounded by

(ii) an *air box* with $\nu = 1/\mu_0$.

The boundary Γ does not therefore coincide with any physical discontinuity.

We consider two geometries for the air box: a cylinder and a sphere. For more details refer to fig. 1.

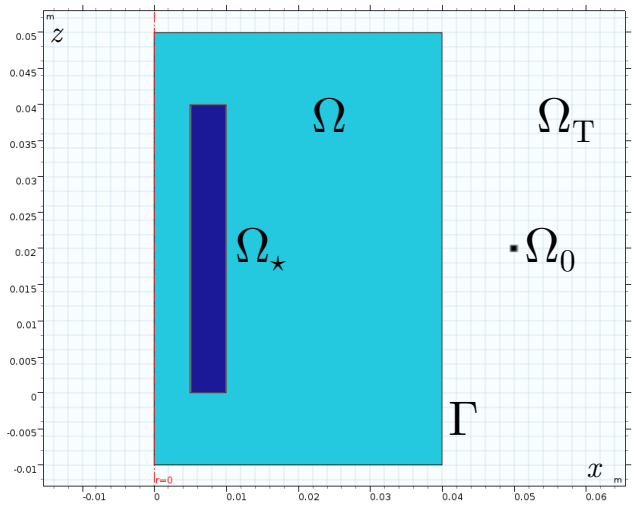

(a) Cylindrical air box with radius 0.04 m and height 0.06 m (the bottom face lies on the plane $z = -0.01\,\mathrm{m}$).

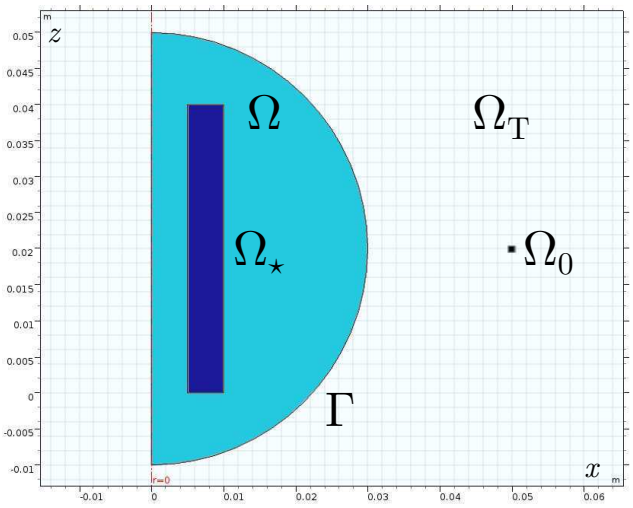

(b) Spherical air box with radius 0.03 m centered in $(0, 0, 0.02\,\mathrm{m})$.

Figure 1: Geometries of Ω and Ω_0 for the axisymmetric example: slices parallel to the positive XZ-plane. The cylinder forming $\Omega_\star$ has radius 0.01 m and height 0.04 m (the bottom face lies on plane $z = 0$), while its cylindrical hole has radius 0.005 m. The circumference on the XY-plane forming Ω_0 (shown as a point in the figures) has radius 0.05 m and lies on the plane $z = 0.02$.

Consequently, for each air box we consider a different configuration of multipoles:

(i) Multipoles up to order 1, i.e. (40) for $\mathsf{l} = 0, \mathsf{m} = 0$ and $\mathsf{l} = 1, \mathsf{m} = -1, 0, 1$, whose centers are uniformly disposed on a cylinder with radius 0.005 m and height 0.026 m (the bottom face lies on plane $z = 0.007\,\mathrm{m}$). The number of centers is set to the (rounded) logarithm of the number of intersections of entities of the primal mesh $\mathcal{M}$ on Γ.

(ii) Multipoles up to order 4, all in the center of the spherical air box. This configuration leads to a diagonal matrix $\mathbf{M}_{\mathrm{T}}$ because of the orthogonality of spherical harmonics [11, p. 108, (3.55)].

Our code is written in `MATLAB R2016b`, using an iterative solver applied to the Schur complement (35). Note that we use an iterative solver not only for its computational efficiency, but also because we have to: with $\omega = 0$, the solution is not unique without a gauge for the magnetic vector potential in Ω, like (26), which we do not impose under the cell method.

The iterative solver used is the *minimum residual method* (`minres`) with a *symmetric successive over-relaxation* preconditioner [26, p. 37, Section 3.3] given by $(\mathbf{D}_{11} + \mathbf{L}_{11})\,\mathbf{D}_{11}^{-1}\,(\mathbf{D}_{11} + \mathbf{L}_{11})^{\mathsf{T}}$, with $\mathbf{D}_{11}, \mathbf{L}_{11} \in \mathbb{R}^{N_{\mathrm{edges}}, N_{\mathrm{edges}}}$ diagonal and lower triangular matrix, respectively, of the top-right block (pure cell method) of (33), i.e. $\mathbf{C}^{\mathsf{T}}\mathbf{M}_\nu\mathbf{C}$. Figure 2 shows the convergence profiles for each configuration of

multipoles: the spherical air box makes the solver achieve the desired tolerance of 10^{-11} slightly faster. The *transpose-free quasi-minimal residual method* (`tfqmr`) also converges with the same preconditioner, but after a few more iterations.

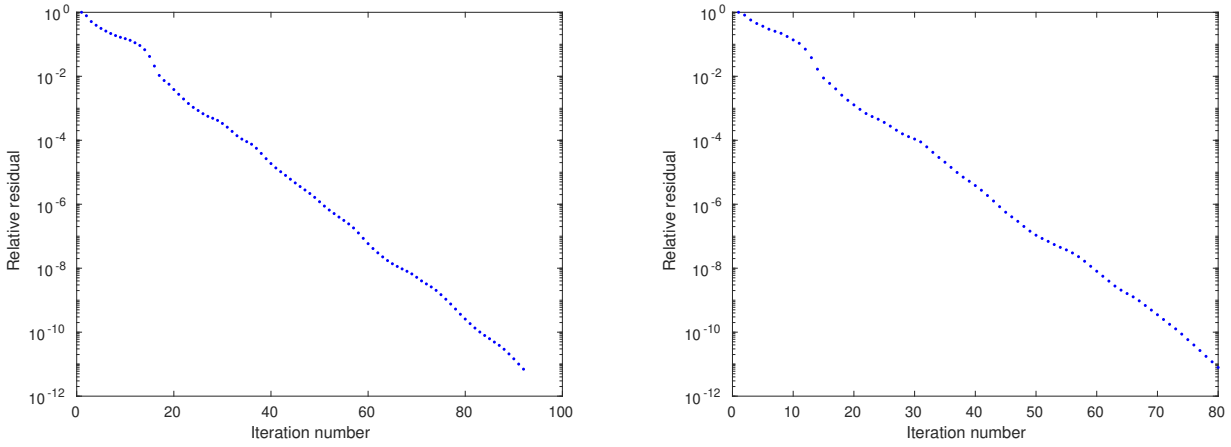

(a) Cylindrical air box with multipoles on internal cylinder. (b) Spherical air box with multipoles in the center.

Figure 2: Plot of relative residual norms vs. iteration numbers for `minres`. Relative residual norms are defined as $\|\mathbf{b} - \mathbf{A}\mathbf{x}_i\|/\|\mathbf{b}\|$ for linear problem $\mathbf{A}\mathbf{x} = \mathbf{b}$, with i iteration number. The y-axis (relative residual norms) is in logarithmic scale.

We test the implementation with a benchmark solution returned by `COMSOL Multiphysics 5.3`, which also provides the meshes. This solution is produced by 3$^{\text{rd}}$-order FEM on a very refined mesh of a spherical air box of radius 0.6 m (20 times larger than the radius of the spherical air box of fig. 1b) centered in $(0, 0, 0.02\,\text{m})$. Dirichlet boundary conditions ($\mathbf{n} \times \mathbf{A} = \mathbf{0}$) are imposed on the air box boundary.

Figures 3 and 4 compare the x and z Cartesian components of the magnetic flux density resulting from the coupling with the benchmark solution. The magnetic flux density is taken along the segment with corners $(0.0075\,\text{m}, 0, 0)$ and $(0.0075\,\text{m}, 0, 0.04\,\text{m})$, which is inside $\Omega_\star$. The accuracy with the benchmark solution for both the cylindical and spherical air box is similar, even if the cylindrical air box is larger than the spherical one.

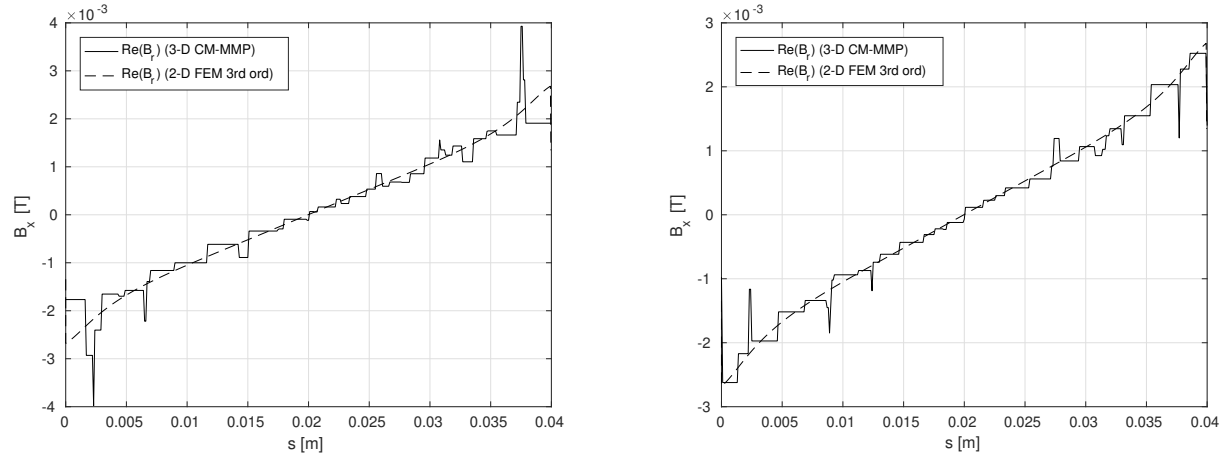

(a) Cylindrical air box with multipoles on internal cylinder. (b) Spherical air box with multipoles in the center.

Figure 3: Value of $\mathbf{B}_x$ along the segment with corners $(0.0075\,\text{m}, 0, 0)$ and $(0.0075\,\text{m}, 0, 0.04\,\text{m})$.

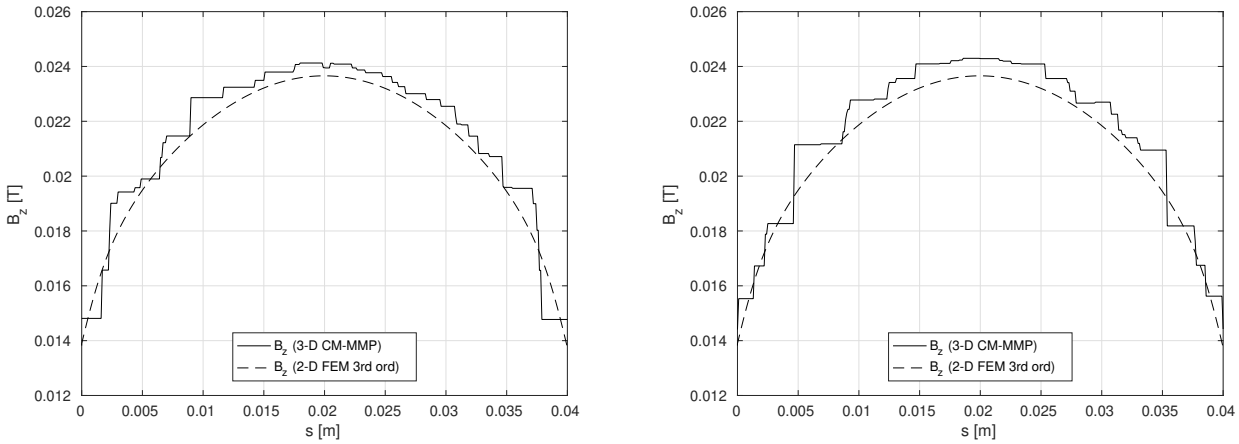

(a) Cylindrical air box with multipoles on internal cylinder.

(b) Spherical air box with multipoles in the center.

Figure 4: Value of $\mathbf{B}_z$ along the segment with corners $(0.0075\,\mathrm{m}, 0, 0)$ and $(0.0075\,\mathrm{m}, 0, 0.04\,\mathrm{m})$.

5. CONCLUSION

The authors are not aware of any prior work addressing the coupling of Trefftz methods with a framework for numerical schemes based on volume meshes like co-chain calculus. We explain for the first time how to formulate a boundary term for this framework that takes into account the exterior problem. The particular case of coupling the cell method with MMP is also presented here for the first time.

Compared to other hybrid approaches that rely on BEM, coupling with a Trefftz method enjoys several advantages [27, p. 51], namely a simpler assembly process, as there are no singular integrals, and exponential convergence when the coupling boundary is far from field singularities. This entails a small number of degrees of freedom for the Trefftz method that permits to compute the Schur complement of the final system.

ACKNOWLEDGMENT

This work was supported by the Swiss National Science Foundation [grant number 2000021_165674/1].

We acknowledge Jasmin Smajic, Institute for Energy Technology, Hochschule für Technik Rapperswil, for putting the authors in contact through a research exchange to the University of Padova.

REFERENCES

1. Ralf Hiptmair. Discrete Hodge operators. *Numerische Mathematik*, 90(2):265–289, December 2001.
2. Ralf Hiptmair. Discrete Hodge-operators: an algebraic perspective. *Progress In Electromagnetics Research*, 32:247–269, 2001.
3. Alain Bossavit. 'Generalized finite differences' in computational electromagnetics. *Progress In Electromagnetics Research*, 32:45–64, 2001.
4. Douglas N. Arnold, Richard S. Falk, and Ragnar Winther. Finite element exterior calculus, homological techniques, and applications. *Acta Numerica*, 15:1–155, May 2006.
5. Anil Nirmal Hirani. *Discrete Exterior Calculus*. PhD thesis, California Institute of Technology, May 2003.
6. Enzo Tonti. A direct discrete formulation of field laws: the cell method. *CMES - Computer Modeling in Engineering and Sciences*, 2(2):237–258, 2001.
7. Enzo Tonti. Finite formulation of electromagnetic field. *IEEE Transactions on Magnetics*, 38(2):333–336, March 2002.

8. Lorenzo Codecasa. Refoundation of the cell method using augmented dual grids. *IEEE Transactions on Magnetics*, 50(2):497–500, February 2014.
9. Federico Moro and Lorenzo Codecasa. Indirect coupling of the cell method and BEM for solving 3-D unbounded magnetostatic problems. *IEEE Transactions on Magnetics*, 52(3):1–4, March 2016.
10. Federico Moro and Lorenzo Codecasa. A 3-D hybrid cell boundary element method for time-harmonic eddy current problems on multiply connected domains. *IEEE Transactions on Magnetics*, 55(3):1–11, March 2019.
11. John David Jackson. *Classical Electrodynamics*. Wiley, New York, NY, 3rd edition, 1999.
12. Lorenzo Codecasa and Francesco Trevisan. Piecewise uniform bases and energetic approach for discrete constitutive matrices in electromagnetic problems. *International Journal for Numerical Methods in Engineering*, 65(4):548–565, September 2005.
13. Federico Moro, Daniele Desideri, Alberto Doria, Alvise Maschio, Cristian Med, and Lorenzo Codecasa. A face-smoothed cell method for static and dynamic piezoelectric coupled problems on polyhedral meshes. *Journal of Computational Physics*, 386:84–109, June 2019.
14. Mario Bebendorf. Approximation of boundary element matrices. *Numerische Mathematik*, 86(4):565–589, October 2000.
15. Ralf Hiptmair, Andrea Moiola, and Ilaria Perugia. *A Survey of Trefftz Methods for the Helmholtz Equation*, pages 237–279. Springer International Publishing, Cham, October 2016.
16. Christian Hafner. Chapter 3 - The Multiple Multipole Program (MMP) and the Generalized Multipole Technique (GMT). In Thomas Wriedt, editor, *Generalized Multipole Techniques for Electromagnetic and Light Scattering*, Mechanics and Mathematical Methods–Series of Handbooks, pages 21–38. Elsevier Science B.V., Amsterdam, September 1999.
17. B. Carrascal, G. A. Estevez, Peilian Lee, and V. Lorenzo. Vector spherical harmonics and their application to classical electrodynamics. *European Journal of Physics*, 12(4):184, July 2000.
18. Pedro R. S. Antunes. A numerical algorithm to reduce ill-conditioning in meshless methods for the Helmholtz equation. *Numerical Algorithms*, 79(3):879–897, November 2018.
19. Daniele Casati and Ralf Hiptmair. Coupling finite elements and auxiliary sources. *Computers & Mathematics with Applications*, 77(6):1513–1526, March 2019.
20. Jasmin Smajic, Christian Hafner, and Juerg Leuthold. Coupled FEM-MMP for computational electromagnetics. *IEEE Transactions on Magnetics*, 52(3):1–4, March 2016.
21. Daniele Casati, Ralf Hiptmair, and Jasmin Smajic. Coupling finite elements and auxiliary sources for Maxwell's equations. *International Journal of Numerical Modelling: Electronic Networks, Devices and Fields*, December 2018.
22. William McLean. *Strongly Elliptic Systems and Boundary Integral Equations*. Cambridge University Press, Cambridge, 1st edition, 2000.
23. Peter Monk. *Finite Element Methods for Maxwell's Equations*. Numerical Mathematics and Scientific Computation. Clarendon Press, Oxford, 1st edition, 2003.
24. Koya Sakakibara. Analysis of the dipole simulation method for two-dimensional Dirichlet problems in Jordan regions with analytic boundaries. *BIT Numerical Mathematics*, 56(4):1369–1400, December 2016.
25. Ralf Hiptmair. Finite elements in computational electromagnetism. *Acta Numerica*, 11:237–339, January 2002.
26. Richard Barrett, Michael Berry, Tony F. Chan, James Demmel, June Donato, Jack Dongarra, Victor Eijkhout, Roldan Pozo, Charles Romine, and Henk Van der Vorst. *Templates for the Solution of Linear Systems: Building Blocks for Iterative Methods*. SIAM, Philadelphia, PA, 2nd edition, 1994.
27. Dimitra I. Kaklamani and Hristos T. Anastassiu. Aspects of the Method of Auxiliary Sources (MAS) in computational electromagnetics. *IEEE Antennas and Propagation Magazine*, 44(3):48–64, June 2002.